

# An Anti CuO<sub>2</sub>-type Metal Hydride Square Net Structure in Ln<sub>2</sub>M<sub>2</sub>As<sub>2</sub>H<sub>x</sub> (Ln = La or Sm, M = Ti, V, Cr, or Mn)\*\*

Hiroshi Mizoguchi,\* SangWon Park, Haruhiro Hiraka, Kazutaka Ikeda, Toshiya Otomo, and Hideo Hosono

**Abstract:** Using a high pressure technique and the strong donating nature of H<sup>−</sup>, a new series of tetragonal La<sub>2</sub>Fe<sub>2</sub>Se<sub>2</sub>O<sub>3</sub>-type layered mixed-anion arsenides, Ln<sub>2</sub>M<sub>2</sub>As<sub>2</sub>H<sub>x</sub>, was synthesized (Ln = La or Sm, M = Ti, V, Cr, or Mn; x ≈ 3). In these compounds, an unusual M<sub>2</sub>H square net, which has anti CuO<sub>2</sub> square net structures accompanying two As<sup>3−</sup> ions, is sandwiched by (LaH)<sub>2</sub> fluorite layers. Notably, strong metal–metal bonding with a distance of 2.80 Å was confirmed in La<sub>2</sub>Ti<sub>2</sub>As<sub>2</sub>H<sub>2.3</sub>, which has metallic properties. In fact, these compounds are situated near the boundary between salt-like ionic hydrides and transition-metal hydrides with metallic characters.

Much research has been devoted to inorganic solids with mixed anions.<sup>[1]</sup> The ordering of anions in layered structures often enhances the low dimensionality of the electronic structure, enabling the development of new compounds with unusual physical properties such as superconductivity.<sup>[2]</sup> For example, LaFeAsO is a prototype iron-based ZrCuSiAs-type (1111-type) superconductor, wherein the LaO blocking layer and FeAs conducting layer are alternately stacked along the c-axis.<sup>[2a]</sup> Recently, mixed-anion compounds containing H<sup>−</sup> ions have been attracting attention. In inorganic solids, the H<sup>−</sup> anion has the following characteristics: 1) the charge is changeable; 2) the size is flexible, depending on the environment; 3) it has an isotropic electronic structure, because of the absence of p character; 4) it is a strong σ donor (using the filled 1s orbital) comparable to CN<sup>−</sup>; and 5) the 1s<sup>2</sup> energy

level is sensitive to the environment.<sup>[3]</sup> Because of these properties, H<sup>−</sup> commonly forms salt-like ionic compounds with positive cations such as alkali-metal or alkaline-earth-metal ions. Recently, several compounds that contain H<sup>−</sup> have been reported in 3d transition metal (TM) oxides.<sup>[4]</sup> Although we have attempted to insert hydrogen into solids with large ionic character, hydrides do not generally have a large formation enthalpy, which is due to the small electron affinity of H. The stability of a hydride is much lower than that of a fluoride, which has a similar lattice size and charge state. Herein, we report the synthesis of novel layered arsenides containing H<sup>−</sup>, using a high-pressure technique. The mixed-anion compounds, Ln<sub>2</sub>M<sub>2</sub>As<sub>2</sub>H<sub>x</sub> (Ln = La or Sm; M = Ti–Mn), which have metallic properties, adopt La<sub>2</sub>Fe<sub>2</sub>Se<sub>2</sub>O<sub>3</sub>-type structures similar to the 1111-type. In this structure, (LaH)<sub>2</sub> and M<sub>2</sub>HAs<sub>2</sub> layers are stacked with each other, and unusual octahedron, MH<sub>2</sub>As<sub>4</sub> with two-short and four-long distortion is seen. The H<sup>−</sup> ion also forms a M<sub>2</sub>H square net with an anti-CuO<sub>2</sub> layer, owing to its isotropic character and the low valence states of the surrounding Ti ions.

The new hydrides, Ln<sub>2</sub>M<sub>2</sub>As<sub>2</sub>H<sub>x</sub> with La<sub>2</sub>Fe<sub>2</sub>Se<sub>2</sub>O<sub>3</sub>-type (2223-type) structures,<sup>[5]</sup> prepared in this study are shown in the Supporting Information, Table S1. The obtained lattice constants and unit cell volumes are given in Figure 1 and the Supporting Information, Table S1. These are the first hydrides to adopt the 2223-type structure. Pellets of all these compounds were black. Attempts to obtain these hydrides without the use of high pressure failed, and attempts to obtain La<sub>2</sub>Fe<sub>2</sub>As<sub>2</sub>H<sub>x</sub> and La<sub>2</sub>M<sub>2</sub>As<sub>2</sub>F<sub>x</sub> (M = Ti, Cr) were also

[\*] Dr. H. Mizoguchi, S.-W. Park,<sup>[†]</sup> Prof. H. Hosono  
Materials Research Center for Element Strategy  
Tokyo Institute of Technology, Yokohama 226-8503 (Japan)  
E-mail: mizoguchi@lucid.msl.titech.ac.jp

Dr. H. Hiraka, Dr. K. Ikeda, Prof. T. Otomo  
Institute of Materials Structure Science  
High-Energy Accelerator Research Organization (KEK)  
Tsukuba 305-0801 (Japan)

[†] Present address: Advanced Functional Thin Films Department  
Korea Institute of Materials Science  
Changwon, 641-831, Republic of Korea

[\*\*] This study was supported by the JSPS FIRST and the JST ACCEL projects. The neutron scattering experiment was approved by the Neutron Scattering Program Advisory Committee of IMSS, KEK (Proposal No. 2014S06). We are grateful to Dr. O. Fukunaga, Dr. Y. Muraba, and Dr. J. Bang (Tokyo Institute of Technology) for help with the high-pressure experiments. We also thank Dr. O. Jepsen and Dr. Y. Nohara (Max Planck Institute, Stuttgart, Germany) for providing the LMTO code.

Supporting information for this article is available on the WWW under <http://dx.doi.org/10.1002/anie.201409023>.

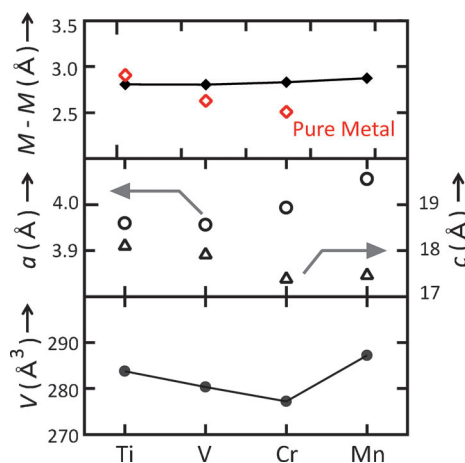


**Figure 1.** Tetragonal unit cell parameters and volumes of La<sub>2</sub>M<sub>2</sub>As<sub>2</sub>H<sub>x</sub> (M = 3d TM). The M–M distances in the *ab* plane (♦) are also shown in comparison with those of pure metal (◇).

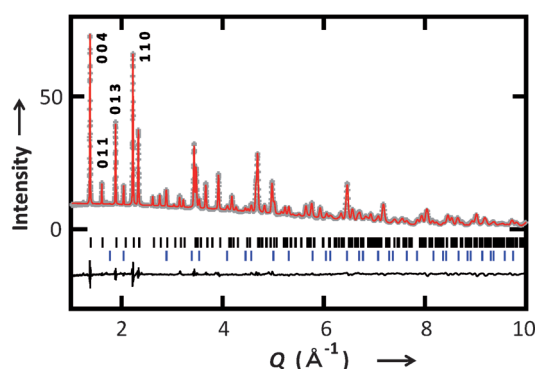


**Figure 2.** Observed (+), calculated (red —), and difference NPD Rietveld profiles for  $\text{La}_2\text{Ti}_2\text{As}_2\text{H}_x$  at 300 K. The vertical bars at the bottom show the calculated positions of the Bragg diffractions of  $\text{La}_2\text{Ti}_2\text{As}_2\text{H}_x$  (upper) and  $\text{LaAs}$  (lower). The estimated amount of  $\text{LaAs}$  was 7.4% by mass.

unsuccessful. The crystal structure of  $\text{La}_2\text{Ti}_2\text{As}_2\text{H}_x$  was refined, using the time-of-flight neutron powder diffraction (TOF-NPD) data, based on a 2223-type structure with the space group  $I4/mmm$  (No. 139). The Rietveld structure refinements are given in Figure 2 (see also the Supporting Information, Table S2 and the CIF). The structure is shown in Figure 3a, and some bond distances are given in the Supporting Information, Table S3. In the layered structure, the  $(\text{LaH})_2$  layer and  $(\text{M}_2\text{HAs}_2)$  layer are alternately stacked along the  $c$ -axis. Although an As–As pair is seen because of the mirror plane ( $z=0$ ), the distance (3.59 Å) is too long for dimer formation. Ti occupies a  $4c$  site with  $D_{4h}$  symmetry, and adopts a  $\text{TiH}_2\text{As}_4$  octahedral coordination with two short and four long distortions (Figure 3b). In the  $ab$  plane, Ti forms a square net (Figure 3c). Specifically, H2 sits on the  $2b$  site with  $D_{4h}$  symmetry, to form an unusual  $\text{Ti}_2\text{H}$  plane, which is the same as the anti- $\text{CuO}_2$  plane seen in cuprate superconductors. Note that the Ti–Ti distance in the net shown in Figure 3c is 2.80 Å, which is shorter than that in  $\alpha$ -Ti with a hexagonal close-packed structure (2.90 Å, Figure 1; Supporting Information, Table S4), indicating strong Ti–Ti direct interactions. Among the obtained compounds, strong metal–metal bonds are observed only for  $\text{M}=\text{Ti}$ . The blocking layer is composed of a  $(\text{LaH})_2$  layer with the fluorite structure, and therefore H1 is coordinated only with La. The refined occupancy factors of H1 and H2 are 0.71 and 0.86, respectively (anisotropic thermal vibration parameters were used for H2). The hydrogen content estimated from the NPD data almost agreed with the value obtained using thermal desorption spectroscopy (TDS), as shown in the Supporting Information, Figure S1. Note that desorption occurs at high temperature, despite the small formation enthalpies of hydrides. The

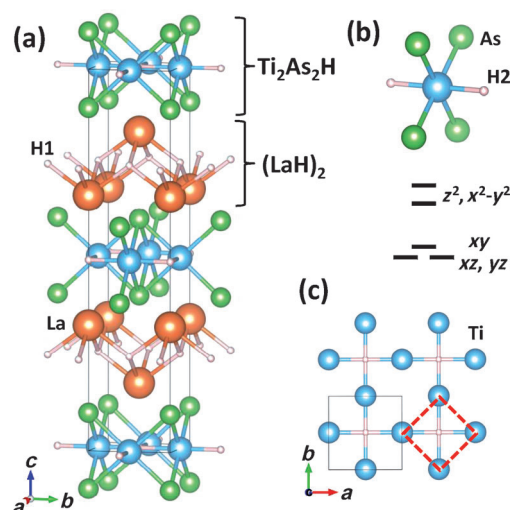


**Figure 3.** a) Crystal structure of layered compound,  $\text{La}_2\text{Ti}_2\text{As}_2\text{H}_{2.3}$ . b) Local coordination around Ti ion, and schematic diagram of energy level of Ti3d orbitals in  $D_{4h}$  symmetry. The Ti–H direction is chosen as the principle axis ( $z$ -axis) of the local orbital coordination system. c)  $\text{Ti}_2\text{H}$  square net; Ti square net is also shown by the red dashed box.

resistivity of  $\text{La}_2\text{Ti}_2\text{As}_2\text{H}_{2.3}$  is  $1.0 \times 10^{-3} \Omega \text{ cm}$  at 300 K, and decreases with decreasing temperature, indicating metallic behavior. No superconducting transition was observed until 1.8 K, as shown in the Supporting Information, Figure S2. The magnetic susceptibility does not show a clear temperature dependence, indicating Pauli paramagnetic behavior.

Figure 4 shows the electronic band structure ( $E$ - $k$  diagram) and density of states (DOS) of  $\text{La}_2\text{Ti}_2\text{As}_2\text{H}_3$ . Two bands cross the Fermi energy ( $E_F$ ) along the  $\Gamma X$  line, indicating a metallic character, which is consistent with the experimental results. In real space, the  $\Gamma$  to  $X$  line corresponds to the  $[110]$  direction. The partial DOS (PDOS, Figure 4, right-hand side) provides the following information about the chemical bonds

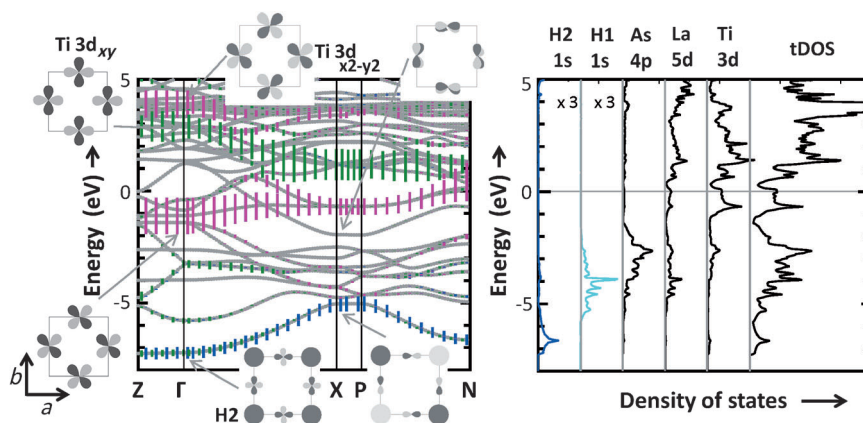


**Figure 4.** Band structure diagram for  $\text{La}_2\text{Ti}_2\text{As}_2\text{H}_3$ ,  $\Gamma = (0,0,0)$ ,  $Z = (1/2, 1/2, -1/2)$ ,  $X = (0,0,1/2)$ ,  $P = (1/4, 1/4, 1/4)$ , and  $N = (0, 1/2, 0)$ . The Brillouin zone is shown in the Supporting Information, Figure S3. The energy scale is defined so that the Fermi energy corresponds to zero energy. The fat-band diagram<sup>[6]</sup> on the left-hand side shows the orbital contributions of H2 1s (blue), Ti 3d $_{x^2-y^2}$  (red), and Ti 3d $_{xy}$  (green). The local orbital coordination system is defined by the Ti square net (Figure 3c, red dashed box), rather than the axis of the crystallographic lattice, to emphasize the direct Ti–Ti bonding. The PDOS is shown on the right-hand side.

in this compound. The La 5d/4f orbitals are located in the region + (0–5) eV, and these are mostly unoccupied, indicating that the La ion is in an approximately trivalent state. Similarly, As adopts a  $-3$  charge state with a  $4p^6$  closed-shell configuration. For H1, which can interact directly with La, bonding parts are seen in the region  $-(5.7\text{--}2.5)$  eV. For H2, bonding parts are seen in the region  $-(7.2\text{--}5.0)$  eV, indicating a different chemical state for these  $H^-$  ions. The bonding part of H2 1s is much deeper than that of As 4p, suggesting that H2 is a stronger donor than H1. H 1s character is also seen for the empty bands (Supporting Information, Figure S4), indicating strong covalency with Ti/La. The splitting between the bonding and antibonding states is 12–13 eV. The  $E$ - $k$  diagram (Figure 4, left-hand side) contains fat bands, denoted by vertical colored lines.<sup>[6]</sup> The contributions of H2 1s, Ti  $3d_{x^2-y^2}$ , and Ti  $3d_{xy}$  are shown by blue, red, and green lines, respectively. Note that the local orbital coordination system is defined by the Ti square net (Figure 3c, red dashed box), rather than the axis of the crystal system, to emphasize the direct Ti–Ti bonding. At the  $\Gamma$  point, interactions between H2 1s and Ti  $3d_{xy}$  form lower bonding ( $-7.2$  eV) and higher antibonding levels, because of the matched symmetry. However, the interaction is non-bonding at the X point. In the place of the H2 1s and Ti  $3d_{xy}$  interaction, a H2 1s–Ti  $4p_x/4p_y$  interaction is possible in the X point (bonding:  $-5.0$  eV). According to the PDOS, the  $DOS(E_F)$  is mainly Ti 3d in character, with a small degree of La 5d character. Although the ten bands originating from Ti 3d near  $E_F$  are complicated, it is possible to understand the band dispersion by considering the Ti square net (Figure 3c). For Ti  $3d_{x^2-y^2}$  bands (red fat bands), Ti–Ti direct interactions are possible at the  $\Gamma$  point; d–d  $\sigma$  bonding and d–d  $\sigma^*$  antibonding states are seen at  $-1.1$  and  $+3.8$  eV, respectively. The splitting (ca. 5 eV) is not large, despite the short Ti–Ti distance. This result can be attributed to the second-neighbor interactions within the net, which compensate for nearest-neighbor interactions. These bands are degenerate at the X point, and lose their chemical interactions. Similarly, the  $d_{z^2}$  and  $d_{xz}/d_{yz}$  bands have appropriate dispersions near  $E_F$  and contribute to the metallic nature;  $d_{xz}/d_{yz}$  bands are also highly stabilized at the X point ( $-1.6$  eV), because the La 5d acts as an acceptor (the contribution of La 5d is not shown in the  $E$ - $k$  diagram). In contrast, the Ti  $3d_{xy}$  orbitals (green fat bands) are highly destabilized in the region  $+(1.1\text{--}3.1)$  eV by  $\sigma$  interactions with H2 1s, which is a strong donor. As a result, the Ti  $3d_{xy}$  orbitals make no contribution to the metallic properties. Salt-like ionic arsenide-hydrides such as  $Ca_5As_3H$  have been reported by Corbett and co-workers.<sup>[7]</sup> The present newly synthesized compounds seem to be located at the boundary region between salt-like ionic hydrides and TM hydrides with metallic characteristics.

First, we discuss the observed local coordination structure of  $La_2Ti_2As_2H_{2.3}$ . H2 adopts an unusual square-planar coordination (HTi<sub>4</sub>, Figure 3c). The features of the local chemical coordination of  $H^-$  ions in intermetallic compounds have been reviewed by Yvon;<sup>[8]</sup> however, to the best of our knowledge, no square planar coordination of  $H^-$  ions has yet been reported. The H ion, which has a small charge, cannot be surrounded by many cations with large positive charges

because of the electroneutrality rule. Therefore, the Ti ion around H2 must have a low valence state. In fact, the Ti ion with two short and four long distortions (TiH<sub>2</sub>As<sub>4</sub>) splits the 3d orbital, as shown in Figure 3b. Although H and As have similar electronegativity values,<sup>[9]</sup> the H ion is strongly coordinated with Ti, which is most likely due to its small size. Compressed octahedra are common in  $(n-1)d^{10}ns^0$  cations such as  $Hg^{2+}$ , where the empty s state acts as an acceptor.<sup>[10]</sup> In the present hydrides, the distorted coordination can be explained by the unusual chemical bonding due to the presence of  $H^-$  as a donor. This idea is supported by the fact that the 2223-type fluorides have not been synthesized. Although fluorides have larger formation enthalpies, as a result of the high electron affinity of F, the  $F^-$  ion is unable to act as a  $\sigma$  donor. Interestingly, Ti<sub>4</sub>Sb<sub>2</sub>H<sub>0.9</sub> reported recently includes a similar Ti<sub>2</sub>H<sub>0.9</sub> net with a Ti–Ti distance of 2.82 Å.<sup>[11]</sup> In this tetragonal layered structure, (Ti<sub>2</sub>Sb<sub>2</sub>) rock-salt layer and Ti<sub>2</sub>H<sub>0.9</sub> layer are stacked along the  $c$ -axis, and the TiH<sub>4</sub>H<sub>2</sub> unit is composed of an elongated octahedron with four short and two long distorted bond lengths ( $4 \times 2.00$  Å,  $2 \times 2.38$  Å).

Next, we discuss the Ti–Ti bonding observed in  $La_2Ti_2As_2H_{2.3}$ . Among the compounds synthesized in this study, this system was the only one to exhibit strong M–M interactions. While other 2223-type compounds, including oxychalcogenides and oxypnictides, have been reported,<sup>[5]</sup> such strong metal–metal bonding has not been observed to date.<sup>[12]</sup> The possibility of direct Fe–Fe interactions in 1111-type LaFeAsO has been pointed out;<sup>[13]</sup> however, the interaction is much weaker than that in  $La_2Ti_2As_2H_{2.3}$ . This difference can be explained by the fact that 1111-type compounds have been limited to  $M = Cr\text{--}Cu$ . Metal–metal bonds formed in early TM compounds often have low oxidation states,<sup>[14]</sup> and do not occur in 1111-type compounds, which often contain late TM ions.

Finally, we discuss the changes in the electronic structure when M is changed from Ti to Mn. As Figure 1 illustrates, a V-shaped curve in the unit cell volumes was observed across the TM series. The following three changes are expected to take place in the electronic structure when M is changed: 1)  $E_F$  shifts to a shallower position, owing to enhanced band-filling; 2) the M 3d band position deepens due to the increase in the core charge of M, causing an increase in energy overlap with the As 4p band. This enhances covalent interactions between M 3d and As 4p; and 3) a decrease in M–M direct interactions narrows the M 3d band.

These effects increase the  $DOS(E_F)$ . The large  $DOS(E_F)$  values seen in  $M = Cr$  and Mn destabilize the non-magnetic state, causing the appearance of magnetic ordering, as observed in LaFeAsO.<sup>[2a]</sup>

In conclusions, new mixed-anion compounds,  $Ln_2M_2As_2H_x$  ( $Ln = La, Sm$ ;  $M = Ti, V, Cr, Mn$ ;  $x \approx 3$ ) were synthesized using a high-pressure technique and taking advantage of the electron-donating power of the  $H^-$  ion. These materials have an  $La_2Fe_2Se_2O_3$ -type layered crystal structure in which (LaH)<sub>2</sub> and (M<sub>2</sub>HAs<sub>2</sub>) layers are alternately stacked. The M<sub>2</sub>HAs<sub>2</sub> layer comprises an anti CuO<sub>2</sub>-type M<sub>2</sub>H layer that is typical of cuprate superconductors. The M square net in this layer exhibits strong direct M–M bonding

in the case of  $M = \text{Ti}$ . These mixed-anion compounds are located at the boundary between salt-like ionic hydrides such as alkali-metal hydrides and TM hydrides with metallic characteristics.

### Experimental Section

The synthesis of polycrystalline samples of  $\text{Ln}_2\text{M}_2\text{As}_2\text{H}_x$  and  $\text{La}_2\text{M}_2\text{As}_2\text{F}_3$  ( $\text{Ln} = \text{La, Sm}$ ;  $M = \text{Ti, V, Cr, Mn}$ ) was attempted by solid-state reactions at high temperatures using a belt-type high-pressure anvil-cell. The starting materials were  $M$  ( $M = \text{Ti, V, Cr, Mn, Fe}$ ; 99.9%),  $\text{LnAs}$  ( $\text{Ln} = \text{La, Sm}$ ; 99.9%),  $\text{La}$  (99.9%), and  $\text{LaF}_3$  (99.9%). Appropriate amounts of these materials were milled in an ethanol suspension for 3 h, dried, and then pressed into pellets. The pellet was placed in an h-BN sleeve with a mixture of  $\text{Ca}(\text{OH})_2$  and  $\text{NaBH}_4$  as the hydrogen source.<sup>[15]</sup> The cell was heated at 1473–1573 K under 2.5–5.0 GPa for 0.5–1.0 h. The chemical compositions of the products were determined using a JXA-8530F electron microprobe analyzer (JEOL). The hydrogen contents were estimated using TDS. The crystal structures of the synthesized materials were determined by powder X-ray diffraction (Bruker D8 Advance TXS) using  $\text{CuK}\alpha$  radiation. For  $\text{La}_2\text{Ti}_2\text{As}_2\text{H}_x$ , TOF-NPD was used to determine the position of H at 300 K; the data were collected, with an exposure time of 2 h, at NOVA (beamline BL21, a decoupled liquid-hydrogen moderator), using the 300 kW spallation neutron source at the Japan Proton Accelerator Complex (J-PARC), Japan. Rietveld refinements of the TOF-NPD patterns were performed using a general structure analysis system (GSAS) code.<sup>[16]</sup> The scattering lengths of La, Ti, As, and H used were  $8.24 \times 10^{-13}$ ,  $-3.44 \times 10^{-13}$ ,  $6.58 \times 10^{-13}$  and  $-3.74 \times 10^{-13}$  cm, respectively. The dependence of the electrical resistivity on temperature was measured over the range 1.8–300 K by a conventional four-probe method. Magnetization measurements were performed using a vibrating sample magnetometer (Quantum Design). Band structure calculations were performed using the linear muffin-tin orbital (LMTO) method, with the atomic sphere approximation, including the combined correction.<sup>[16]</sup>

Received: September 12, 2014

Revised: October 18, 2014

Published online: November 10, 2014

**Keywords:** high-pressure chemistry · hydrides · metal–metal interactions · mixed anion phases · titanium

- [1] S. J. Clarke, P. Adamson, S. J. C. Herkelrath, O. J. Rutt, D. R. Parker, M. J. Pitcher, C. F. Smura, *Inorg. Chem.* **2008**, *47*, 8473.
- [2] a) Y. Kamihara, T. Watanabe, M. Hirano, H. Hosono, *J. Am. Chem. Soc.* **2008**, *130*, 3296; b) M. Rotter, M. Tagel, D. Johrendt, *Phys. Rev. Lett.* **2008**, *101*, 107006.
- [3] P. Atkins, T. Overton, J. Rourke, M. Weller, F. Armstrong, *Shriver and Atkins Inorganic Chemistry*, 5th ed., Oxford, **2009**.
- [4] a) R. M. Helps, N. H. Rees, M. A. Hayward, *Inorg. Chem.* **2010**, *49*, 11062; b) Y. Kobayashi, et al., *Nat. Mater.* **2012**, *11*, 507; c) J. Bang, S. Matsuishi, H. Hiraka, F. Fujisaki, T. Otomo, S. Maki, J. Yamaura, R. Kumai, H. Hosono, *J. Am. Chem. Soc.* **2014**, *136*, 7221.
- [5] a) J. M. Mayer, L. F. Schneemeyer, T. Siegrist, J. V. Waszczak, B. Van Dover, *Angew. Chem. Int. Ed. Engl.* **1992**, *31*, 1645; *Angew. Chem.* **1992**, *104*, 1677; b) H. Kabbour, E. Janod, B. Corraze, M. Danot, C. Lee, M.-H. Whangbo, L. Cario, *J. Am. Chem. Soc.* **2008**, *130*, 8261; c) R. H. Liu, Y. A. Song, Q. J. Li, J. J. Ying, Y. J. Yan, Y. He, X. H. Chen, *Chem. Mater.* **2010**, *22*, 1503; d) D. G. Free, N. D. Withers, P. J. Hickey, J. S. O. Evans, *Chem. Mater.* **2011**, *23*, 1625; e) T. Yajima, K. Nakano, F. Takeiri, J. Hester, T. Yamamoto, Y. Kobayashi, N. Tsuji, J. Kim, A. Fujiwara, H. Kageyama, *J. Phys. Soc. Jpn.* **2013**, *82*, 013703.
- [6] O. Jepsen, A. Burkhardt, O. K. Andersen, Program TB-LMTO-ASA, Version 4.7, Max Planck Institute für Festkörperforschung, Stuttgart, **1999**.
- [7] a) E. A. Leon-Escamilla, J. D. Corbett, *J. Alloys Compd.* **1994**, *206*, L15; b) E. A. Leon-Escamilla, J. D. Corbett, *Chem. Mater.* **2006**, *18*, 4782.
- [8] K. Yvon, *Chimia* **1998**, *52*, 613.
- [9] A. L. Allred, E. G. Rochow, *J. Inorg. Nucl. Chem.* **1958**, *5*, 264.
- [10] J. K. Burdett, *Chemical Bonding in Solids*, Oxford **1995**.
- [11] H. Wu, A. V. Skripov, T. J. Udovic, J. J. Rush, S. Derakhshan, H. Kleinke, *J. Alloys Compd.* **2010**, *496*, 1.
- [12] Short Ti–Ti distances (2.86–2.91 Å) have been reported in  $(\text{SrF})_2\text{Ti}_2\text{Pn}_2\text{O}$  ( $\text{Pn} = \text{As, Sb, or Bi}$ ).<sup>[5c,e]</sup> These originates from  $\text{Ti}^{3+}$  with a small ionic size.
- [13] K. Suzuki, H. Usui, S. Iimura, Y. Sato, S. Matsuishi, H. Hosono, K. Kuroki, *Phys. Rev. Lett.* **2014**, *113*, 027002.
- [14] P. A. Cox, *Transition Metal Oxides*, Oxford, **1995**.
- [15] a) M. Iwamoto, Y. Fukai, *Mater. Trans. JIM* **1999**, *40*, 606; b) Y. Muraba, S. Matsuishi, H. Hosono, *Phys. Rev. B* **2014**, *89*, 094501.
- [16] A. C. Larson, R. B. Von Dreele, *General Structure Analysis System (GSAS)*; Los Alamos National Laboratory Report LAUR 86-748; Los Alamos National Laboratory: Los Alamos, NM, **2004**.